



Experimental investigation of electric propulsion systems using C12A7 electrified hollow cathodes

Norman Gondol¹ · Martin Tajmar¹

Received: 25 January 2022 / Revised: 29 March 2022 / Accepted: 30 March 2022 / Published online: 16 May 2022
© The Author(s) 2022

Abstract

The development and experimental investigation of two low-power electric propulsion concepts using compact heaterless C12A7 electrified (C12A7:e-) hollow cathodes is presented. The first concept represents an electrothermal thruster, in which a cathode discharge is used to heat a gas that is subsequently accelerated in a nozzle-shaped anode. The second propulsion system is an attempt to develop a sub-500 W magnetoplasmadynamic thruster (MPDT) that uses a rectangular discharge channel that allows to increase the applied magnetic field and thus lower the necessary discharge current. Extensive parameter studies with both concepts were conducted, and the thrust and discharge properties of different geometric and operational configurations were determined. This work is a follow-up publication of a previous paper (Gondol and Tajmar in CEAS Space J 14:65–77, 2021).

Keywords C12A7 · Electric propulsion · Electrothermal propulsion · Electromagnetic propulsion

1 Introduction

C12A7:e- is a promising emitter material for heaterless hollow cathodes as several studies have suggested a very low work function and chemical stability at room temperature [1–3]. However, the exact thermionic emission properties have been the subject of debate as the published work functions span from 0.6 eV [2, 3] to more than 2 eV [4].

Research on C12A7:e- hollow cathodes is being conducted at Technische Universität Dresden (TUD). The experiments have resulted in compact devices that allow heaterless operation and reliable long-term electron emission [5], opening the possibility to actively use the cathodes in different low-power electric space propulsion concepts. In this context, two propulsion systems have been developed and extensively tested. This publication is intended to present the latest thruster iterations and the results of a testing campaign. The target thrust levels of both concepts were defined to be in the high micronewton to low millinewton range at a power

level below 500 W. Section 2 introduces the electrothermal thruster and presents the results of the respective test series. Section 3 elaborates on the design and testing of the MPDT.

2 Electrothermal thruster

2.1 Previous work

The idea of a micronewton electrothermal hollow cathode thruster (HCT) was first introduced by Gessini at the University of Southampton (UoS) [6]. The thruster concept was mainly based on early observations of high energetic ions that were measured in hollow cathode plasma plumes by various researchers [7, 8]. These high energetic ions were seen as contributors to a notably higher thrust of an ordinary hollow cathode compared to the thrust generated by the gas flow through the cathode, making hollow cathodes attractive as possible stand-alone thrusters [6]. Subsequently, tests were carried out on the space-qualified hollow cathode of the T6 gridded ion thruster, using an indirect thrust measurement setup [9]. First tests with the thrust stand showed good agreement of the cold gas thrust measurements with theoretical predictions, but thermal effects during discharge operation impeded an accurate thrust measurement [10]. An improvement of the test setup resulted in the first thrust

✉ Norman Gondol
Norman.Gondol@tu-dresden.de
Martin Tajmar
Martin.Tajmar@tu-dresden.de

¹ Institute of Aerospace Engineering, Technische Universität Dresden, Dresden, Germany

measurements of the hollow cathode during discharge using argon as the working gas. The measured thrust reached up to 2.4 mN and was well above the thrust expected by the efflux of heavy particles (ions and neutrals) at a temperature on the order of the cathode wall temperature [11], indicating additional heating and thrust production mechanisms. The thrust signal clearly showed an increase with the discharge current, indicating a similar operational principle to arcjets. Moreover, an additional potential thrust contribution by magnetoplasmadynamic phenomena was hypothesized.

A more elaborate test series with argon and krypton at discharge currents between 5 and 25 A was conducted and confirmed the previous findings. At a 25 A discharge, the I_{sp} was on the order of 300 s with argon and 240 s with krypton at thrust levels between 1 and 6 mN [12]. The test results showed that a simple thermalization of the gas in the orifice with the orifice walls was not sufficient to explain the high I_{sp} that could be measured. In further studies, Gessini et al. improved the performance of the thruster by narrowing the orifice diameter [12].

Grubisic expanded the research on the HCT to the smaller T5 hollow cathode and investigated the impact of the anode configuration. The use of a conical instead of a cylindrical anode was identified as being beneficial for reducing the discharge voltage and maintaining spot mode operation [13].

Frollani then conducted the first effort to derive an analytical performance model of a hollow cathode thruster and derived an optimized version of the T5 and T6 HCTs in which the keeper was replaced by a nozzle-shaped anode and an additional external magnetic field generated by a solenoid was implemented. Moreover, the indirect thrust measurement was replaced by a direct thrust measurement using a pendulum thrust balance. The HCT using the smaller T5 cathode was tested at currents up to 2.5 A, resulting in a thrust range of 0.2–0.7 mN and an I_{sp} between 100 and 140 s. The larger T6 cathode was operated at currents up to 24 A, yielding a thrust of up to 2.61 mN and an I_{sp} of up to 323 s. Although thrust and I_{sp} could be improved, the thrust efficiency of the device was on the order of 1–2%, which is unattractive for space applications [14].

2.2 Principle of operation

As stated, the operational principle of the electrothermal HCT could be identified to be comparable to that of an arcjet propulsion system. The discharge current of a hollow cathode is drawn from the insert to a nozzle-shaped anode that is attached to the cathode assembly. The current carried by the plasma is heating the gas mainly by Ohmic heating, and frequent CEX collisions additionally increase the neutral gas temperature which approaches an equilibrium with the ion temperature within the cathode, as suggested by various 2D modeling efforts [15, 16].

Due to the narrow dimensions in the orifice, the current density and resistive heating reach their maximum in the orifice region, resulting in high gas temperatures. The cathode interior pressure is generally orders of magnitude higher than the environmental pressure. It is thus likely for the heavy particle species (ions and neutrals) to reach supersonic conditions in the orifice. The supersonic gas then enters the nozzle region and likely experiences an expansion and acceleration. The gas flow in the cathode tube can be well described by a continuum flow at a large distance from the orifice, but the continuum assumption loses validity at the orifice entrance and shortly after the orifice region, where the flow quickly transitions to a free molecular flow as the plasma and neutral densities rapidly decrease [17]. This constraint indicates that only a fraction of the nozzle contributes to the acceleration of the gas, as the effect of the nozzle is greatly reduced in a free molecular flow regime. However, test results by Grubisic showed that using a nozzle-shaped anode instead of a cylindrical or flat anode improved the performance of the device, indicating a beneficial effect of a conical nozzle shape on the particle acceleration [13].

The efforts made at UoS led to the derivation of several thrust production mechanisms (see f.e. Ref. [14]) that can be exploited to maximize the performance of an HCT. The most straightforward mechanism is the gas dynamic thrust, i.e., the momentum and pressure contribution of heavy particles $F_{h,gas}$, which can be expressed by:

$$F_{h,gas} = \dot{m}_i u_i + \dot{m}_n u_n + (p_i + p_n - p_0), \quad (1)$$

where \dot{m}_i , u_i and p_i are the ion mass flow rate, exit velocity and exit pressure, respectively, \dot{m}_n , u_n and p_n are the neutral mass flow rate, exit velocity and exit pressure, respectively, p_0 is the ambient pressure and A_{ex} is the exit area. Analogously, the gasdynamic thrust contribution of electrons $F_{e,gas}$ can be stated. In contrast to the heavy particles, the vast majority of electrons, apart of the electrons that are dragged to the outside by the exiting ions, are collected by the anode and thus do not contribute to the overall momentum flow leaving the thruster, but their pressure term can be written as:

$$F_{e,gas} = (p_e - p_0)A_{ex}. \quad (2)$$

As hollow cathode plasmas show electron temperatures in the low electron volt range (1 eV = 11,605 K) at number densities on the order of $1e20 \text{ m}^{-3}$ in the orifice, the electron pressure term proves to be non-negligible, as shown by Grubisic [13].

In addition to gas dynamic particle contributions, an electromagnetic thrust component can be considered. The current that is drawn from the insert through the orifice to

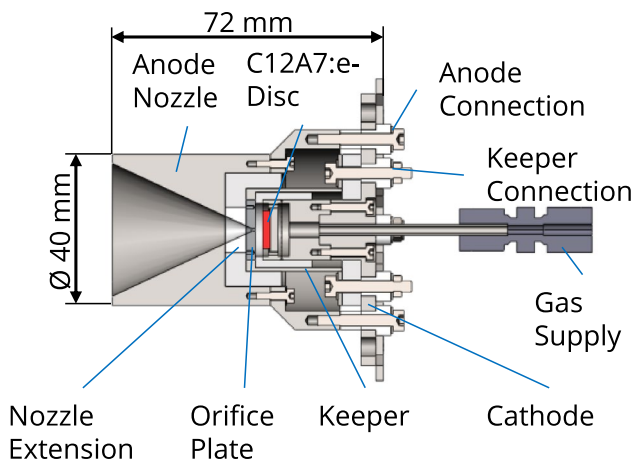


Fig. 1 Cross-section of the electrothermal thruster prototype

the anode induces an azimuthal magnetic field that causes a Lorentz force on the charge carriers. Frollani points out that there are two distinct regions in the hollow cathode, where an electromagnetic force acts on the charge carriers [14]. As the maximum discharge current in this study is limited to 3 A, the overall electromagnetic force is considered to be negligible. Moreover, high-energy ions have been seen as an additional thrust mechanism. As stated in Sect. 2.1, many experiments have shown ions in the cathode plume with energies above the discharge voltage. Frollani estimated the total thrust contribution of high-energy ions in a 16 A discharge to be merely on the order of $4 \mu\text{N}$ [14]. This contribution is likely even lower in thrusters operating at lower currents.

For a low current device, the stated thrust mechanisms narrow down almost entirely to a gas dynamic thrust characteristic of the HCT and thus an arcjet-like behavior.

2.3 Testing prototype

The electrothermal thruster prototype is schematically depicted in Fig. 1.

The thruster consists of a welded cathode assembly made of stainless steel that serves as the gas distributor and as the electrical connection of the insert. The electron-emitting insert is a C12A7:e- disc with a diameter of 10 mm and a width of 2 mm. The emitter is attached to the downstream end of the cathode using an electrically conductive silver adhesive. An electrical insulation made of the machinable Rescor ceramic separates the cathode body from the keeper assembly. The keeper consists of a welded steel part and the orifice plate, which is made of molybdenum to withstand the high temperatures that can occur in the orifice region.

Two different orifice geometries were considered, one with a 0.4 mm and one with a larger 0.8 mm orifice diameter. The orifice was designed with a straight part at the upstream



Fig. 2 Thruster prototype with a 25° nozzle

end and a diverging part with the same angle as the anode nozzle. The length of the straight part was set to 0.5 mm, as an overly long orifice did not yield the desired effects in preliminary tests [1]. A thread around the orifice plate circumference allows a connection of the steel component with the orifice plate. The nozzle extension downstream of the orifice plate serves as electrical insulation between the keeper and the anode nozzle and is made of Rescor. The anode nozzle is made of stainless steel. Three different nozzle geometries with divergence half-angles of 15° , 25° , and 35° were considered for the test series. The assembled thruster prototype is shown in Fig. 2 with the 25° half-angle nozzle.

2.4 Test Results

The test series of the electrothermal thruster was conducted with the same test equipment and methodology as described in Ref. [1] using a 100Ω pre-resistor for the anode and a 150Ω pre-resistor for the keeper to increase discharge stability. For the main test series, the influence of the propellant and the orifice diameters were first investigated using the 25° nozzle and an additional molybdenum content in the C12A7:e- discs of 10%. The molybdenum is intended to increase thermal stability and improve the electrical conductivity of the emitter. The tests were carried out using both krypton and argon. In Fig. 3, the discharge voltage is plotted as a function of the mass flow rate and the discharge current with the 0.4 mm diameter orifice for argon and krypton.

The discharge voltages for both krypton and argon are on the order of 50–60 V for mass flow rates $> 0.4 \text{ mg/s}$, which is relatively high compared to commonly used hollow cathodes. Highly optimized cathodes usually operate at 15–30 V [18–20]. Tests with different C12A7:e- cathodes at TUD showed slightly lower voltages of 30–40 V [5]. The voltage is similar to the voltage obtained using a cylindrical anode and an additional test using an external anode yielded similarly high voltages. The discharge voltage can therefore not necessarily be attributed to the conical shape of the anode and to the anode being in direct proximity to the orifice exit but seems to be a feature of the cathode setup.

Fig. 3: 0.4 mm diameter orifice discharge voltage (note the different scales)

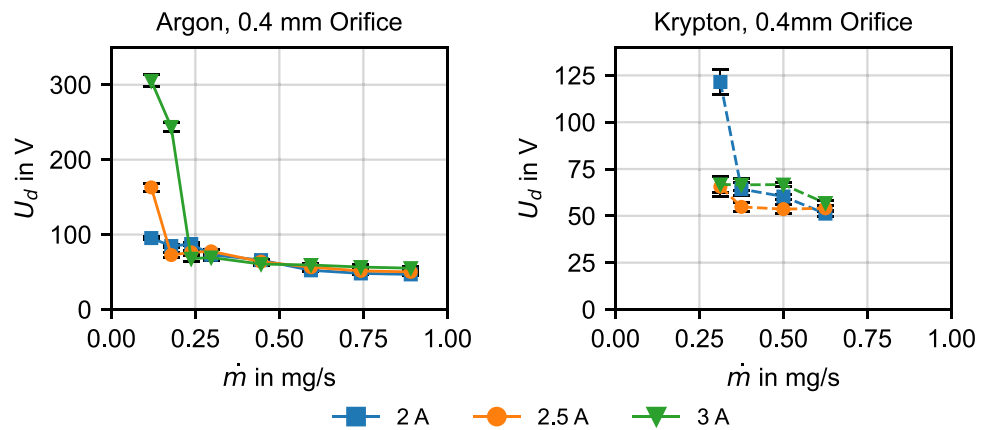
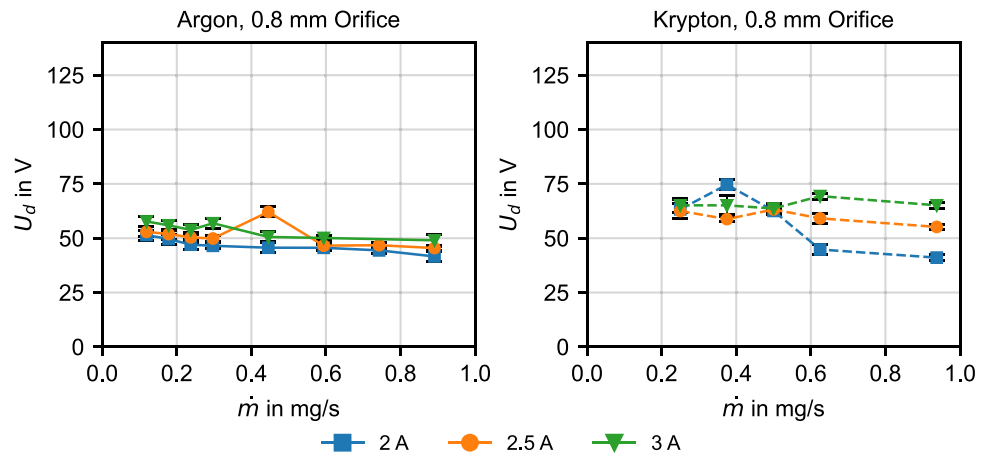


Fig. 4: 0.8 mm diameter orifice discharge voltage



Decreasing the mass flow rate from 0.9 mg/s to approximately 0.3 mg/s using argon leads to a gradual increase of the voltage from around 50 V to 70 V. Below 0.2 mg/s using argon, the voltage increases notably, indicating the transition to a noisy plume mode. Similarly, the krypton discharge transitions to a higher voltage below 0.4 mg/s at a 2 A current. Below 0.3 mg/s, no stable discharge could be achieved using krypton. The argon discharge could be sustained to significantly lower mass flow rates. The discharge voltage for the large orifice is illustrated in Fig. 4. The voltage using the larger orifice shows a light decrease in discharge voltage for argon and a more stable operation at mass flow rates as low as 0.1 mg/s. For krypton, the voltage is in a similar range as with the smaller orifice and slightly higher than the argon discharge, which is unexpected considering the higher ionization potential of argon. Changes in mass flow rate also have a slightly higher influence on the voltage level for krypton.

The measured thrust for the 0.4 mm diameter orifice is shown in Fig. 5 and for the 0.8 mm diameter orifice in Fig. 6. The thrust level using argon increases with discharge current, indicating an increased propellant temperature. For mass flow rates above 0.2 mg/s, the thrust rises nearly

linearly with mass flow rate. At a discharge current of 3 A, lowering the mass flow rate below 0.2 mg/s resulted in a steep increase in thrust, coinciding with the increase in voltage and transition to plume mode operation. The voltage rises to promote ionization as the discharge is starved of the neutral gas atoms resulting in a higher electron temperature.

An increase in orifice electron temperature then results in a higher electron pressure and electron thrust contribution according to Eq. (2), but also in increased heating of the heavy particles by electron collision. The achievable thrust using argon in the covered spectrum of operating points ranges between 0.2 mN up to 0.9 mN. For krypton, the thrust is notably lower and mostly linear to the mass flow range. The thrust measurement shows that using argon is beneficial to increase the performance of the thruster, as the enthalpy of lighter gases can be more easily converted into directed kinetic energy. For the 0.8 mm diameter orifice, the increase in thrust with current and mass flow rate is also evident. The thrust levels here are slightly lower compared to the narrower orifice, which was also observed by Frollani [14], and can be attributed to a less efficient resistive heating of the gas. As no significant voltage increase was observed, an increase of thrust at low mass flow rates is also not visible.

Fig. 5: 0.4 mm diameter orifice thrust measurement

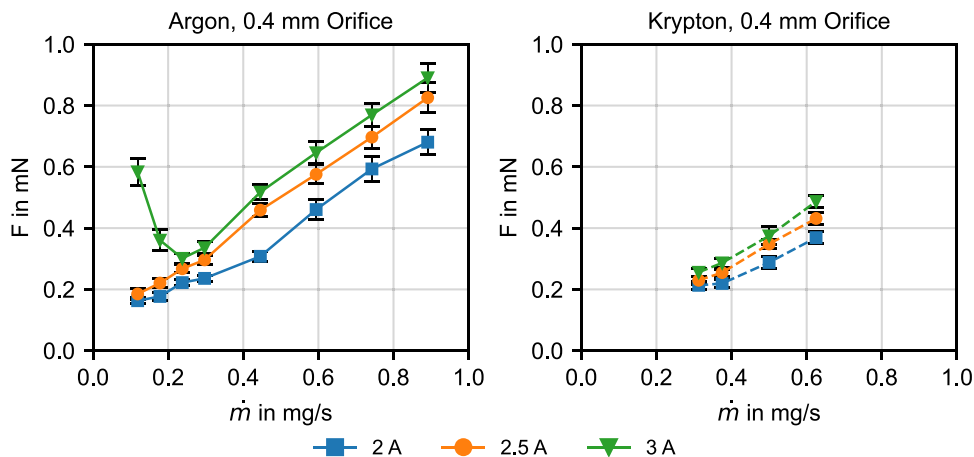


Fig. 6: 0.8 mm diameter orifice thrust measurement

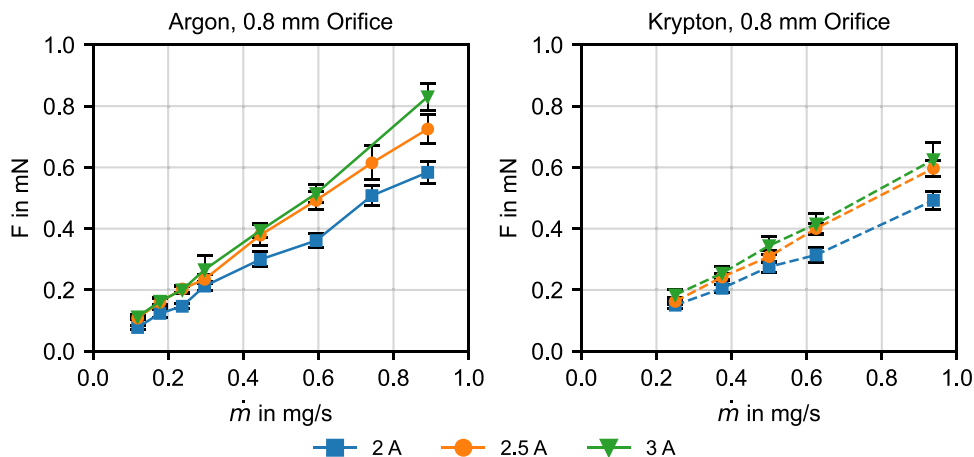
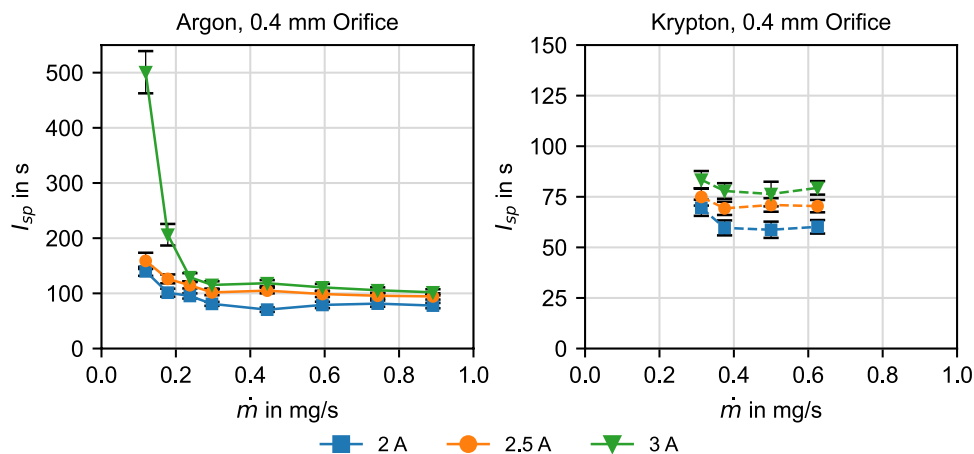
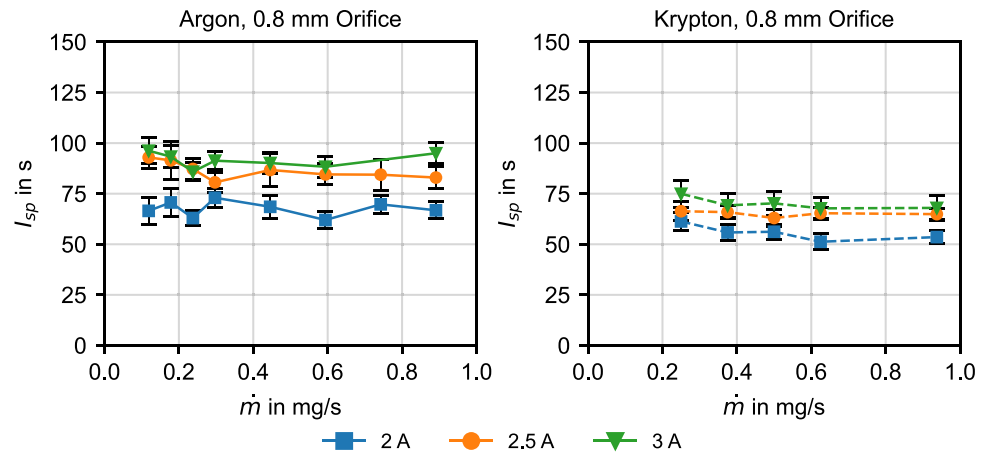
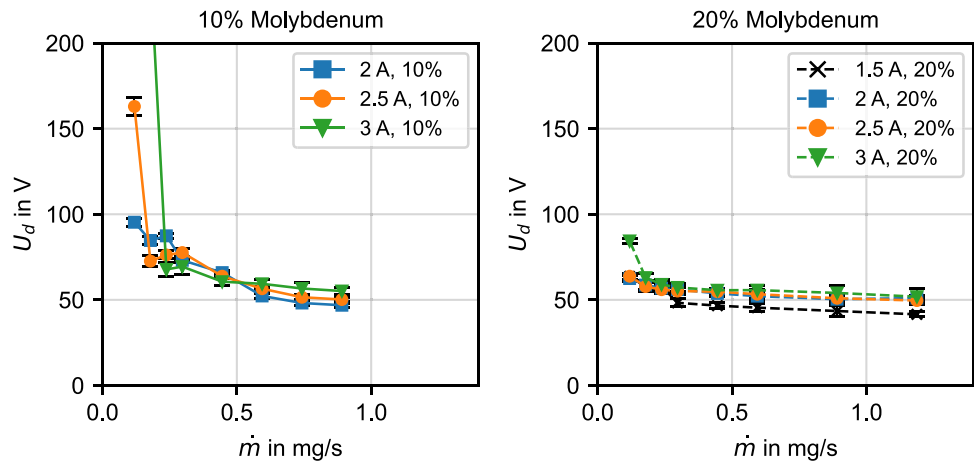


Fig. 7: 0.4 mm diameter orifice I_{sp}



The I_{sp} for the 0.4 mm diameter orifice is shown in Fig. 7 and for the 0.8 mm diameter orifice in Fig. 8. The I_{sp} for the smaller orifice and argon is on the order of 100 s and roughly stable across the covered mass flow rate range above 0.2 mg/s. At lower mass flow rates, the I_{sp} increases slightly for the 2 and 2.5 A discharges and rapidly for the 3 A discharge up to 500 s, which again can be attributed to the increase in voltage and thrust. For krypton, the I_{sp}

is on the order of 60 s – 80 s which is an increase of about 100% compared to simple cold gas operation, but very low for an EP system. The wider orifice results in an even lower I_{sp} for both argon and krypton. Here, the achievable I_{sp} for argon ranges between 60 and 90 s, and for krypton between 50 and 75 s. As the I_{sp} is unsatisfactory, the main focus on optimizing the device should be on improving the I_{sp} .

Fig. 8: 0.8 mm diameter orifice I_{sp} **Fig. 9** Influence of molybdenum content on discharge voltage

The thrust efficiency η_T of an electric propulsion system is defined as:

$$\eta_T = \frac{F}{2\dot{m}P_{el}} \quad (3)$$

with P_{el} being the electric power. The comparatively high discharge voltages and low thrust levels result in a very low thrust efficiency of below 1%, similar to the concepts developed at UoS.

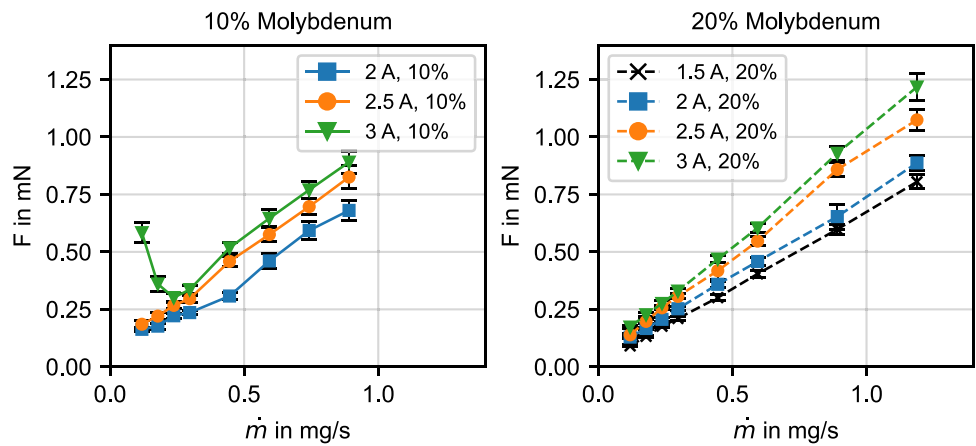
The test results show that using argon and a smaller orifice is superior to the use of krypton and the larger orifice. In contrast to the tested prototypes in the previous publication [1], the 0.4 mm diameter orifice also did not show signs of erosion or clogging during the tests and is thus deemed compatible with the cathode design.

In an effort to reduce the discharge voltage the influence of the molybdenum content was examined. Here, a molybdenum content of 20% in the C12A7:e- emitter was additionally tested with an orifice diameter of 0.4 mm using argon. A comparison of voltage and thrust for 10% and 20% molybdenum contents is shown in Fig. 9 and Fig. 10. While

the voltages using the 20% molybdenum emitters are on the same order of 50 V, the discharge is much more stable even at lower currents. Using the 10% emitters, the voltage starts notable increasing below 0.5 mg/s, whereas the voltage stays nearly constant for mass flow rates as low as 0.2 mg/s using the 20% emitters. Moreover, lower discharge currents could be achieved using the higher molybdenum contents, indicating an overall improved discharge behavior. The thrust lies on the same order for both configurations. Consequently, the I_{sp} does not change notably depending on the molybdenum content in spot mode. The higher content does not show the steep increase in thrust and I_{sp} for very low mass flow rates, as the voltages remain relatively low and stable before the discharge simply extinguishes without transitioning into a high voltage operational mode. The tests showed that a higher molybdenum content does not increase the performance by reducing the discharge voltage but increases the discharge stability significantly and enables operation at lower currents.

The influence of the nozzle geometry is examined next, where tests using argon, a 0.4 mm diameter orifice, and 20% molybdenum content emitters were used. The discharge

Fig. 10 Influence of molybdenum content on thrust



voltages for the three different nozzle half-angles are shown in Fig. 11.

The nozzle geometry has a notable effect on the discharge behavior of the thruster. Using the smallest divergence angle of 15° , the voltage stays relatively stable across the covered mass flow range with voltages between 40 and 55 V. A general trend of increasing voltage with increasing current can be seen, but the 2 A discharge is an exception and shows slightly higher voltages. The lowest current level of 1.5 A is associated with the lowest discharge voltage. Increasing the discharge current yields higher voltages, which is uncommon for hollow cathodes. The increase in voltage with current is nearly linear. A larger half-angle of 25° shows slightly increased voltage levels and a gradual increase as the mass flow rate is reduced. In the 35° nozzle, this trend is amplified and the voltages reach up to 70 V above 0.5 mg/s. The thruster plume did not visibly change for all divergence angles at mass flow rates above 0.5 mg/s but transitioned to a bright plume at operating points coinciding with a strong increase in voltage. The transitional behavior was, however, not examined in detail which generally requires

measurements using an oscilloscope. The 2 A discharge in the 35° nozzle repeatedly showed the highest voltages in the tested current range, indicating a different plasma state or an anomaly. The exact influence of the nozzle shape on the discharge behavior is difficult to quantify. Grubisic argued that a conical anode shape reduces the loss of neutrals in the vicinity of the orifice, and thus increases the local neutral density and ionization [13]. The subsequently increased plasma density resulted in a reduced discharge voltage in the T5 HCT. A higher nozzle divergence angle was seen as advantageous due to the larger electron collecting surface area. The effect of a reduced discharge voltage compared to cylindrical anode shapes could not be seen in the TUD HCT, which might indicate a deviating discharge behavior of C12A7:e- cathodes from conventional hollow cathodes. The reasons for the unique trends in the measured current-voltage characteristics are unknown. The electric circuit consisting of the pre-resistors and power supplies may have a distinct influence on the discharge behavior because the used power supplies are in general not suited for plasma

Fig. 11 Influence of nozzle divergence angle on discharge voltage

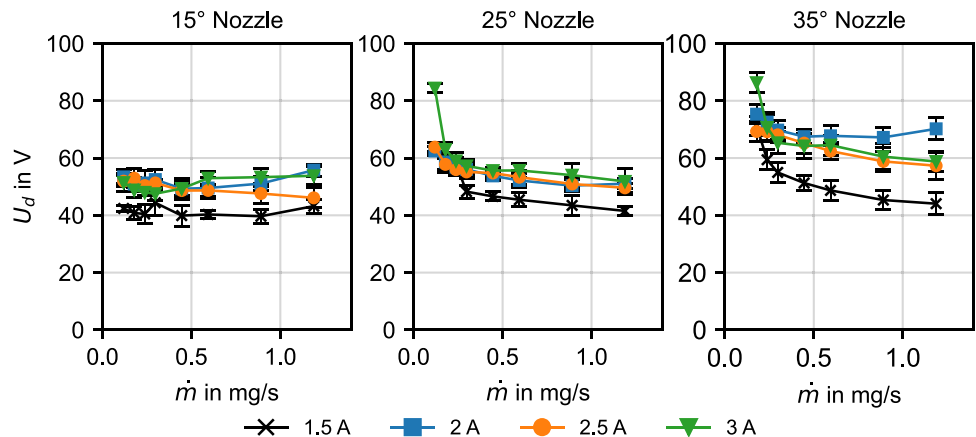
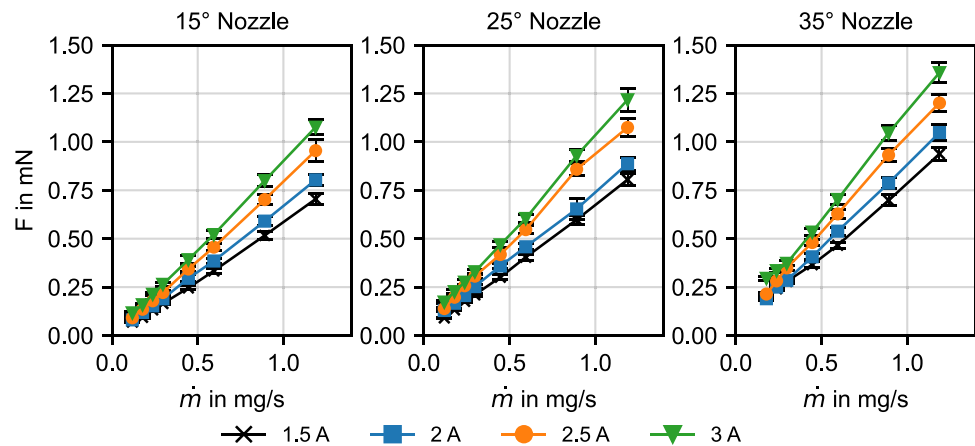


Fig. 12 Influence of nozzle divergence angle on thrust



discharges and showed difficulties during the ignition process using other EP systems developed at TUD.

The measured thrust as a function of the different nozzle divergence angles is shown in Fig. 12.

A clear trend of increasing thrust with increasing nozzle half-angle is evident. The 25° nozzle reaches thrust levels up to 12% higher than the 15° nozzle, and the 35° again improves the thrust by roughly 12% compared to the 25° nozzle. For mass flow rates on the order of 1.2 mg/s, the thrust reaches up to 1.35 mN with the 35° half-angle. The maximum reached I_{sp} is on the order of 120 s for the mass flow rate range where the voltage stays relatively constant. The performance improvement with a larger nozzle can partly be attributed to the increase in voltage which results in a more pronounced electron contribution, but also possibly to an improvement in gas expansion and acceleration. Overall, the tests showed that a higher divergence angle is likely advantageous for this thruster concept.

3 Electromagnetic thruster

3.1 Background

Common MPDTs need several kiloamps of discharge current and consequently power levels in the high kilowatt range to generate a strong azimuthal self-induced magnetic field that results in a strong electromagnetic acceleration of the discharge plasma. Frequently used electron emitters are tungsten rod cathodes that can reliably supply the

necessary current but also pose the main lifetime limiting factor as they are prone to erosion. Typical MPDTs thus are limited to lifetimes on the order of 2000–8000 h [21]. Hollow cathodes have thus been identified as a viable alternative because they can provide both high current levels and long operational lifetimes. Fradkin et al. [22], for example, used a lithium-fueled hollow cathode in a 25 kW MPDT and found the operation with the hollow cathode to be superior compared to conventional rod cathodes in terms of current stability, proneness to erosion, and rapid ignition capability. Toki et al. also conducted a parameter study with different hollow cathode geometries in a hydrogen-fueled thruster and found no significant disadvantage in performance compared to solid cathodes [23]. Besides using more durable electron emitters, the miniaturization of MPDTs into lower power regimes has also been investigated by various researchers in different ways. In the Japanese Electric Propulsion Experiment (EPEX), a hydrazine-fueled pulsed MPDT was tested in orbit with an allocated discharge power of 430 W [24]. Here, the thruster was operated with current pulses of 6 kA with a pulse width of 150 μ s and a frequency of 0.5–1.8 Hz. Toki et al. [25] also investigated the possibility to adopt the operational principle of common applied-field MPDTs to a 1 kW thruster. At low mass flow rates, the thruster plume showed the characteristic bright plasma pinch, called “cathode jet”, which is indicative of an electromagnetic acceleration. One drawback of this approach is the necessity to cool the solenoid using a closed water cycle, which adds complexity. A similar design was presented by Ichihara et al. [26] where an axisymmetric applied-field MPDT was operated at

10–20 A using a hollow cathode, finding an electromagnetic dominated acceleration by the applied magnetic field and an I_{sp} ranging between sub-1000 up to 2000s. Ichihara et al. also presented a design variation where the discharge channel was not axisymmetric but had a rectangular cross-section. The magnetic field here was generated by strong permanent magnets and the current provided by a hollow cathode was limited to 15 A [26, 27]. Here, the I_{sp} reached up to 2600 s with an efficiency of up to 11%.

3.2 Operational principle

Operating common axisymmetric applied-field MPDTs at lower power levels still necessitates strong electromagnets that consume additional power and need to be cooled to prevent overheating. This approach is thus considered not to be suitable for the presented study. Ichihara's concept of using a rectangular discharge channel cross-section is more promising in this context. A rectangular discharge channel has one major advantage: an external magnetic field can be explicitly applied perpendicularly to an electric current. This way, the applied magnetic field directly contributes to the downstream accelerating Lorentz force. In an axisymmetric configuration, the predominantly axial applied magnetic field mainly leads to a swirl motion of the plasma that can partly be converted into an axial acceleration in a magnetic nozzle. Moreover, a strong applied magnetic field can also result in an azimuthal Hall current that can create additional blowing and pumping thrust components [28]. However, for the magnetic field to contribute directly to the downstream accelerating Lorentz force, the magnetic field lines would need to follow an azimuthal path which is not possible from a constructional standpoint in classical axisymmetric designs. The rectangular configuration of a Lorentz force accelerator has been explored extensively in so-called magnetohydrodynamic (MHD) propulsion systems that have been developed mainly for maritime propulsion and proved to work on a large scale [29, 30]. An adaptation to plasma devices for space applications has up to now only been attempted by Ichihara et al. An illustration of the operational principle of the thruster concept presented in this work is shown in Fig. 13.

Within a rectangular, electrically insulating discharge channel, two electrodes are placed on two opposing sides

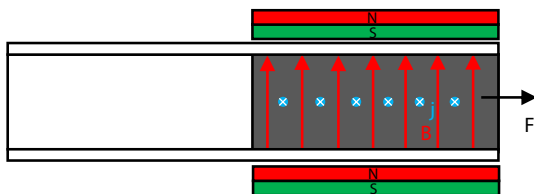


Fig. 13 Operational principle of the electromagnetic thrust concept

of the channel. An external magnetic field is applied perpendicularly to the expected current between the electrodes. Gas is then let into the channel and a breakdown is achieved by applying a high voltage between the electrodes. The generated plasma column serves as the electrical conductor between the electrodes. Due to the perpendicular magnetic field, the Lorentz force acts on the charge distribution in the channel, accelerating both electrons and ions in the downstream direction. The ejected stream of charged particles is thus quasi-neutral and an additional neutralizer is not necessary.

In this configuration, permanent magnets can be used to generate substantially higher magnetic fields compared to electromagnets without consuming additional electric power. A stronger magnetic field allows for the reduction of the discharge current to sustain the same accelerating electromagnetic force. Moreover, the design is easily scalable, and the performance can be adjusted by altering the current and the magnetic field strength of the permanent magnets. Combining this concept with a compact hollow cathode as the electron source can be attractive to additionally increase the lifetime of the MPDT.

Approximating the plasma inside the MPDT as a single electrically conductive fluid, the thrust caused by the electromagnetic acceleration of the charged particles can be estimated by the electromagnetic volume force acting on the plasma, neglecting the influence of the walls. The ideal Lorentz force $F_{L,ideal}$ in this case is simply given by:

$$F_{L,ideal} = I_d w B, \quad (4)$$

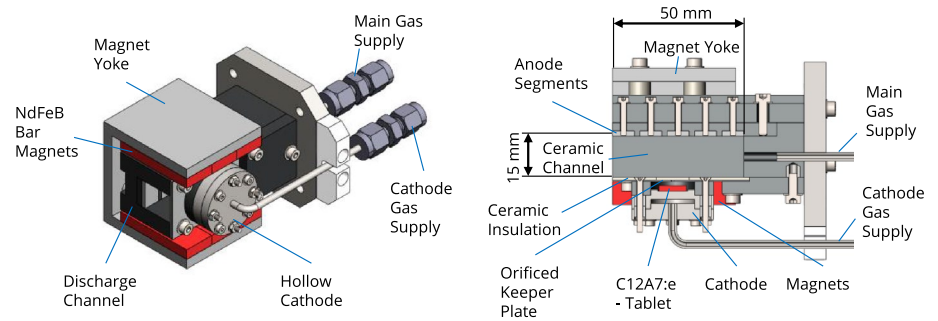
where w is the distance between the electrodes and B is the magnetic flux density. Here, it is assumed that the current density vector is colinear with the electric field vector and perfectly orthogonal to the external magnetic field vector, resulting in a perfectly downstream-pointing force vector. Additional to the electromagnetic thrust, an electrothermal contribution increases the overall thrust, as the gas is heated by the current.

3.3 MPDT prototype

A schematic of the MPDT prototype is shown in Fig. 14.

The rectangular discharge channel is made of Rescor. The hollow cathode assembly is made of stainless steel and uses a C12A7:e- disc emitter. The keeper electrode is a rectangular molybdenum plate that also serves as a sidewall of the discharge channel. An additional ceramic insulation plate made of the machinable Macor ceramic is placed in front of the keeper to avoid direct contact of the plasma with the keeper electrode. Ichihara et al. [27] investigated the influence of a ceramic cover in front of the keeper and noticed a strong erosion pattern and sputtering of the keeper electrode

Fig. 14 MPDT prototype isometric view (left) and cross-section (right)



as the cover was removed. Moreover, the thruster showed a slight decrease in thrust without the cover. Threaded inserts in the channel ceramic provide the means to attach the hollow cathode to the channel. The anode is divided into five segments that can be individually operated. By adjusting the current limits of the individual segments, the effective current density vector can be optimized to reduce the thrust vector skewing that is caused by the Hall effect. Operating the segments individually likely necessitates complex PUs and control loops to adjust the discharge behavior at different operating points. The thruster is equipped with two separate gas supplies, one for the hollow cathode operation and one to additionally provide sufficient gas pressure inside the discharge channel to promote ionization and supply the main discharge. The magnetic field is generated by an array of N40 grade neodymium–iron–boron (NdFeB) bar magnets that are attached to a magnet yoke made of low-carbon steel, acting as a horseshoe magnet. The bar magnets were chosen mainly because of their availability and low price. NdFeB magnets generate very strong magnetic fields but have the drawback of having a very low maximum operating temperature on the order of 80 °C. The magnet assembly thus has very little physical contact with the rest of the thruster to minimize thermal conduction but radiated heat from the channel or the cathode to the magnets still might pose a problem. At the upstream end of the thruster, a stainless steel mounting provides the means to attach the thruster to the thrust balance.

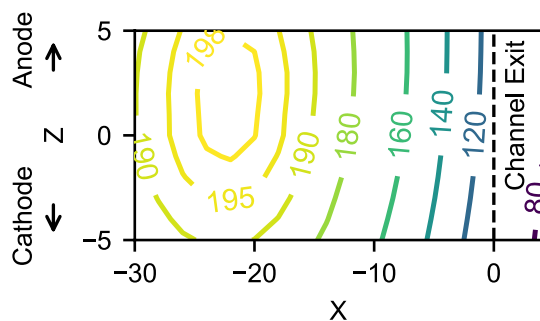


Fig. 15 Magnetic field measurement of the MPDT

A magnetic field measurement using a magnetometer showed good agreement with a magnetic field simulation. In Fig. 15, the measurement data are plotted, where $Z=0$ denotes the centerline. It is evident that the magnetic field is significantly lower at the channel exit, decreasing from a peak flux density of approximately 200 mT 25 mm upstream of the exit plane to 120 mT at the channel exit. This might lead to deviations from the ideal Lorentz force and a complex plasma behavior due to the magnetic field gradients. Due to constructional constraints, this deficit was accepted.

The use of a hollow cathode has an additional drawback in this configuration. Even without deflection of the current density vector from the electric field vector by the magnetic field, the current is expected to spread across the anode surfaces which again leads to a deviation from the ideal acceleration. This could be mitigated using a single very small anode directly opposite of the hollow cathode orifice. However, the power input would be very high, leading to high thermal loads. Moreover, a minimum anode size is necessary to collect the demanded current, otherwise, the cathode will operate in a highly erosive plume mode. It is also suspected that a smaller anode would lead to a narrower ionization zone in the channel, which could result in insufficient ionization and discharge instabilities. Higher mass flow rates would thus be necessary to provide a sufficient neutral density to sustain the discharge. A new approach to lower the spreading of the current was developed for the presented thruster, which represents a novelty. Here, a keeper plate with multiple orifices along the thrust axis was considered that might lead to a more homogeneous current injection. For the test series, a single orifice keeper with a 1 mm diameter orifice as well as different multi-orifice keeper plates were manufactured. The different keepers were laser-cut from a 0.5 mm molybdenum sheet. The multi-orifice keeper has a total of 5 orifices distributed in the axial direction. Preliminary tests showed that only an orifice diameter of 0.4 mm in the multi-orifice keepers resulted in a stable operation. The manufactured thruster prototype is shown in Fig. 16.

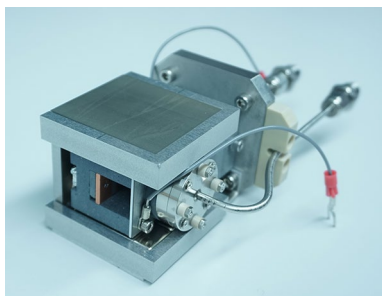


Fig. 16 MPDT testing prototype

3.4 MPDT test results

The test series covered a parameter study to investigate the influence of the cathode position, keeper configuration, magnetic field, and channel dimensions on the performance. The testing followed a fixed procedure. Before each test, the thrust balance was calibrated using a voice coil. The obtained conversion factor was then used to translate the deflection signal of the thrust balance into a thrust value. The ignition process for the individual operating points was initialized from a zero-deflection state by adjusting the desired cathode and discharge channel mass flow rates. As a constant cold gas deflection level was reached, a voltage of 600 V was applied to both the keeper and the anode, leading to a gas breakdown. The operating points were then kept constant for up to 10 s to obtain a stable deflection signal of the torsion thrust balance was achieved. After that, the voltage and gas supplies were disengaged to obtain a new reference zero-deflection measurement. This procedure was repeated for each operating point. Analogous to the electrothermal HCT, a 100 Ω resistor was used for the anode and a 150 Ω resistor for the keeper to enable a stable discharge. A preliminary test showed that for a 150 Ω keeper pre-resistor the minimum current necessary to achieve the

main discharge was 0.8 A. Lower keeper currents resulted in very unstable keeper and anode discharges. For the performance test series, the keeper current was thus kept at a constant 0.8 A during operation. A current range between 2 and 3 A was tested. Below 2 A, no stable discharge could be achieved, and higher currents than 3 A resulted in a strong glowing of the anode segments, indicating temperatures exceeding the thermal limitations of the employed materials. For the parameter study, it was decided to use krypton as the propellant.

In the following, the test results on the influence of the cathode position and keeper configuration with a fixed channel width of 15 mm and height of 14 mm are presented. During the tests, the anode segments were electrically connected to reduce the number of necessary power supplies. In Figs. 17 and 18, the thrust F , I_{sp} , discharge voltage U_d , and efficiency η are plotted as functions of the mass flow rate, discharge current, and cathode position for a single orifice hollow cathode with a diameter of 1 mm. The *Middle* position of the cathode corresponds to a distance of 22 mm upstream of the channel exit, while the cathode is moved 7 mm further downstream in the *Front* position.

For the derivation of the I_{sp} , the sum of the cathode and the discharge channel mass flow rates was used. For the calculation of the efficiency the power necessary to operate the keeper was not included in the calculation. This way, the efficiency is more representative of the thruster performance and can be used to evaluate the potential of the concept. By including the C12A7:e- cathode, which is itself still at a low technological maturity level, the efficiency is worsened and can be misleading.

In Fig. 17, it is evident that the thrust increases linearly with discharge current, as expected by the Lorentz force. The mass flow rate has little influence on the overall thrust, indicating that the electromagnetic thrust is significantly higher than the gas dynamic thrust. The thrust achieved with a single orifice ranges between 2 and 5 mN. Moving the

Fig. 17 Thrust and I_{sp} as a function of the cathode position using a single orifice keeper

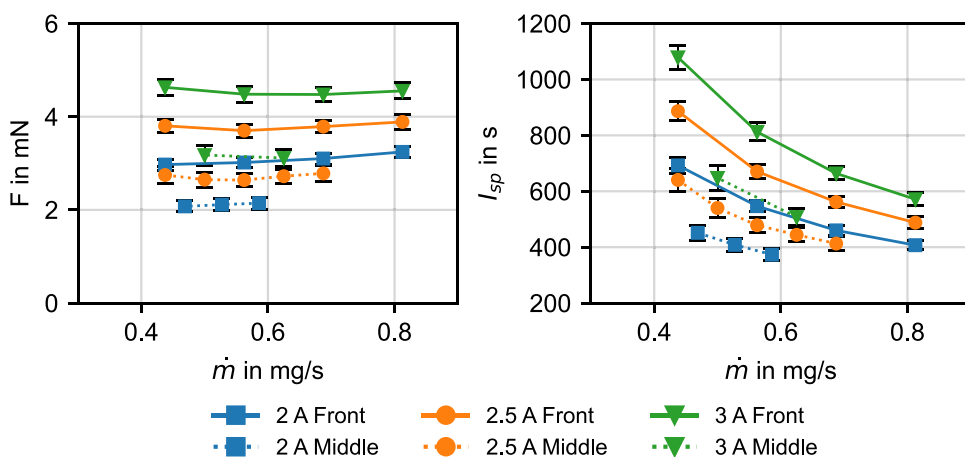
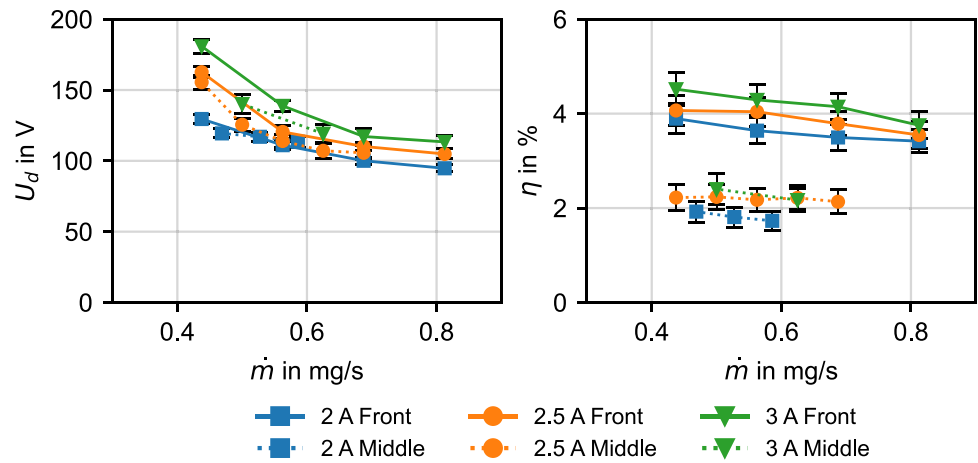


Fig. 18 Discharge voltage and efficiency as a function of the cathode position using a single orifice keeper



cathode further downstream notably increases the achievable thrust by up to 50%. This might be attributed to the lowered wall exposure of the plasma. A slight deviation of the ideal downstream acceleration of charged particles leads to a transverse component of the Lorentz force that accelerates the particles onto the channel walls, transferring a part of their momentum. This effect can be partly mitigated by moving the cathode to the downstream end. The I_{sp} shows a similar trend regarding the position of the cathode. The achievable I_{sp} using a single orifice lies in a range of 400 up to 1100 s. Moving the cathode to the front of the channel significantly increases the achievable I_{sp} . As evident, the I_{sp} also increases as the mass flow rate is reduced, due to the inverse proportionality of both parameters. The discharge voltage in Fig. 18 ranges between 100 and 180 V and shows a slight increase with discharge current and also increases with decreasing mass flow rate. As the mass flow rate is reduced, the plasma discharge is slowly starved of potential charge carriers. A higher voltage is thus necessary to accelerate electrons and promote ionization. The voltage in the front position is slightly higher compared to the middle position. The power demand of the thruster (not considering

the keeper power consumption) is in the range of 200 W at a 2 A discharge and up to 550 W at a 3 A discharge. The keeper power throughout the test series was on the order of 20 W. The relatively high discharge power results in a comparatively low thrust efficiency. For the middle position of the cathode, the efficiency lies on the order of 2%, while the efficiency is increased by moving the cathode to the front to approximately 4%.

In Figs. 19 and 20, the influence on the test results of a multi-orifice keeper in the middle position is shown compared to the single orifice. The thrust in shows an improvement of approximately 20% using the multi-orifice compared to the single orifice. It is thus likely, that either the resulting Lorentz force vector is better aligned with the thrust axis using the multi-orifice or momentum losses are reduced. Hence, the corresponding I_{sp} also shows a significant improvement compared to the single orifice. However, it is evident in Fig. 20 that the multi-orifice keeper increases the voltage demand by approximately 10–25%, depending on the operating point. The overall thrust efficiency shows a slight improvement using the multi-orifice due to the

Fig. 19 Thrust and I_{sp} . Single orifice vs. multiple orifice keeper in middle position

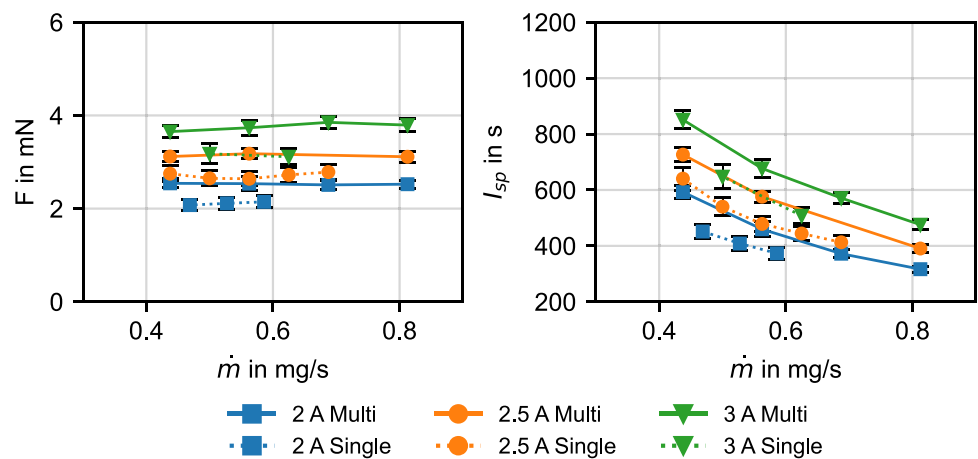
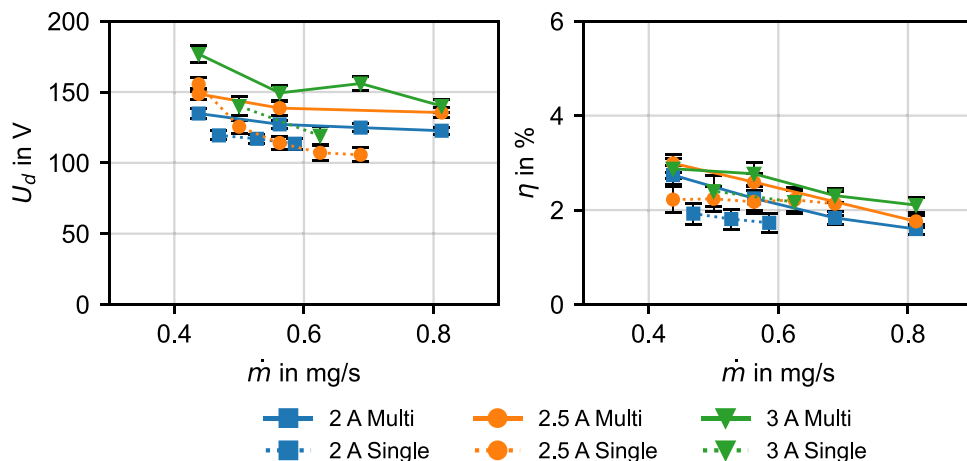


Fig. 20 Discharge voltage and efficiency. Single orifice vs. multiple orifice keeper in middle position



increase in thrust but the improvement is small due to the power increase.

The test results using the multi-orifice in the front cathode position are compared to the single orifice in Figs. 21 and 22. Again, the multi-orifice keeper shows an increased thrust and I_{sp} compared to the single orifice. The thrust reaches up to 5 mN at a 3 A discharge. The corresponding I_{sp} approaches 1200 s. In contrast to the middle position, the voltage is not significantly increased. Using the multi-orifice in the front position allows operating the thruster with a thrust efficiency of over 5%, and thus represents the best performing configuration tested with the fixed benchmark channel geometry.

Using the multi-orifice in the front position, the influence of the channel geometry is examined next. In Fig. 23, the test results for a channel height of 17 mm compared to the 14 mm of the benchmark channel are shown. The channel height does not significantly affect the performance and discharge characteristics of the MPDT. The 3 A discharge for the higher channel extinguished at a higher mass flow rate compared to the lower channel. This might be attributed to the larger discharge volume and thus lower channel pressure,

necessitating higher mass flow rates. The discharge voltage slightly increases by approximately 5% with the higher channel.

The channel width is a geometric parameter that directly influences the electromagnetic force acting on the plasma. Altering the channel width thus implies a change in thruster performance. Using a wider anode-keeper spacing of 17 mm to increase the Lorentz force, however, did not lead to a stable anode discharge. Here, the discharge was characterized by rapid and unstable electric breakdowns between the cathode and the anode. Instead, a narrower channel with a width of 12 mm was tested to investigate the influence of the channel width, summarized in Fig. 24.

A reduction of the electrode spacing from 15 to 12 mm reduces the ideal Lorentz force by 20% for a constant current and magnetic field, according to Eq. (4). This trend can be seen in the test data. The narrower channel results in a 15–30% lower thrust and consequently I_{sp} , consistent with the findings by Ichihara et al. [27]. The discharge voltage is increased notably in the narrower channel, especially for the 3 A discharge, resulting in a reduction of the efficiency of 2–3% compared to the 15 mm channel width. The increase

Fig. 21 Thrust and I_{sp} . Single orifice vs. multiple orifice keeper in front position

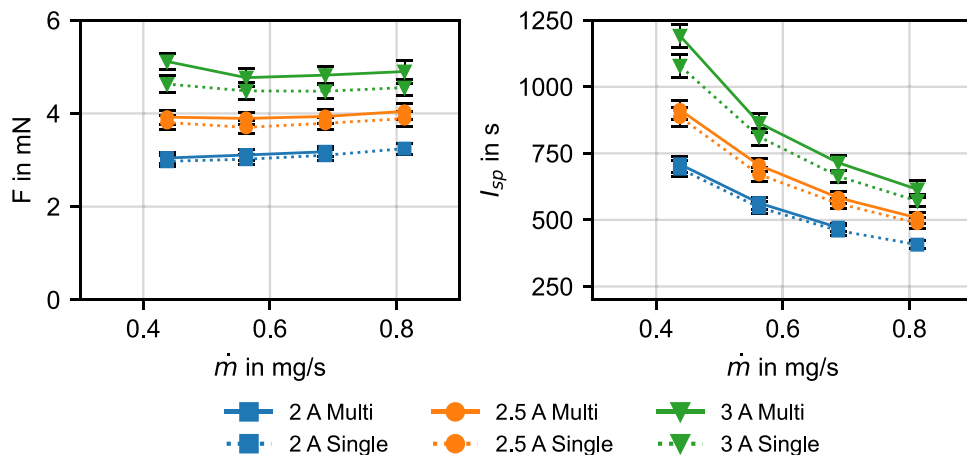


Fig. 22 Discharge voltage and efficiency. Single orifice vs. multiple orifice keeper in front position

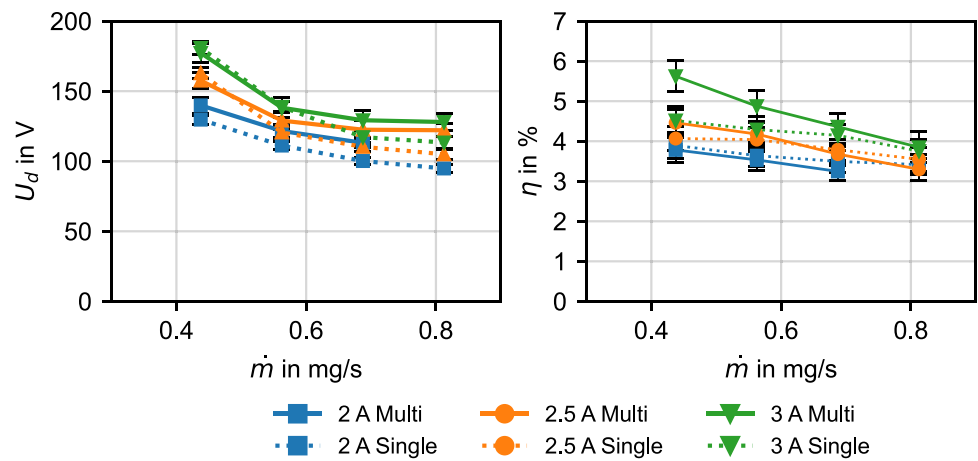


Fig. 23 Influence of the channel height on thrust and discharge voltage

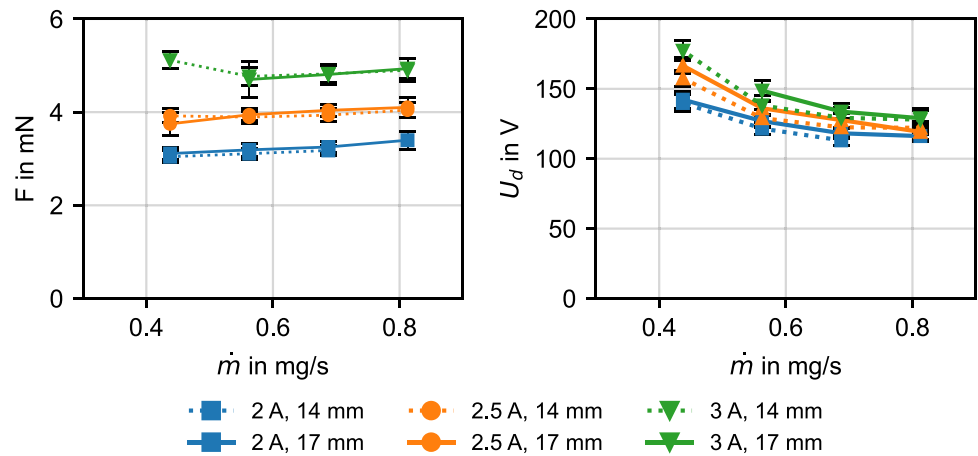
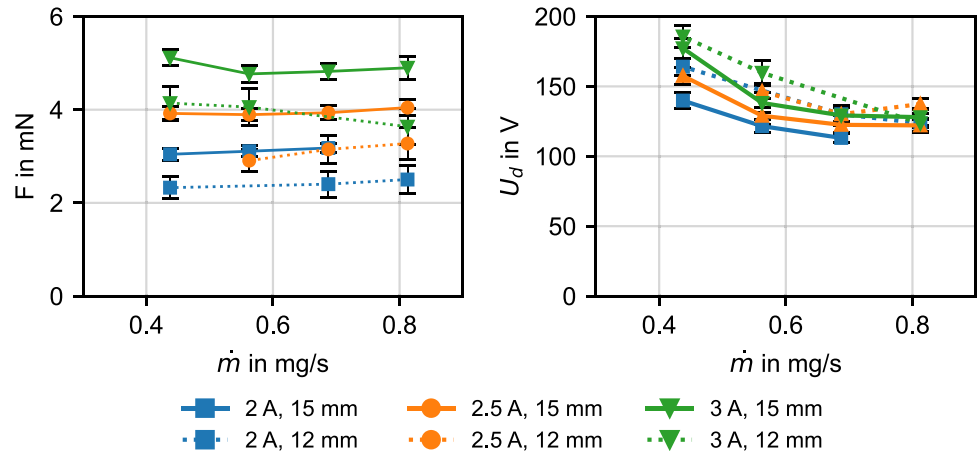


Fig. 24 Influence of the channel width on thrust and discharge voltage

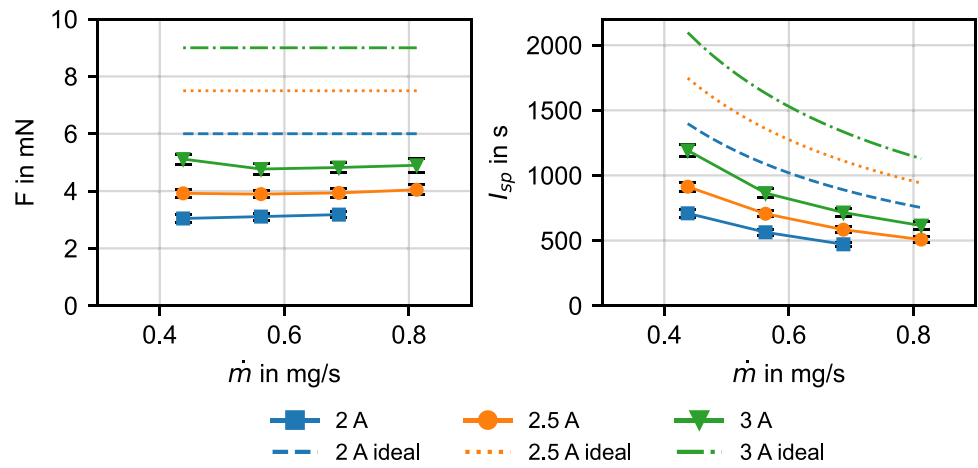


in discharge voltage was not seen by Ichihara et al. Here, a reduction of the channel width was accompanied by a notable reduction of the discharge voltage. The test results show that a wider channel is preferable but increasing the channel width too far leads to discharge instabilities.

In general, the thrust generated by the device is notably lower compared to the ideal Lorentz force, shown for the

multi-orifice in the front position in Fig. 25. Here, the measured thrust and I_{sp} are merely 50–65% of the ideal Lorentz force, assuming a magnetic flux density of 0.2 T. Again, this might partially be attributed to the particle momentum loss to the walls and the skewing of the thrust vector. Additionally, the magnetic field measurement in Fig. 15 showed a significantly lower magnetic flux density

Fig. 25 Thrust and I_{sp} of the MPDT compared to the ideal Lorentz force acceleration



in the front of the discharge channel of 120–150 mT. As the cathode is moved to the front of the channel, a larger part of the current will thus experience a lower magnetic flux density. The measured thrust corresponds to a Lorentz force of approximately 0.11 T, which is closer to the measured magnetic field near the channel exit. Moving the magnet assembly further downstream to increase the peak flux density in the front part of the channel was not successful, because the overlapping part of the magnets experienced high levels of plasma exposure and spark discharges on the magnet surfaces. Furthermore, the anode discharge could not be stably achieved. The most promising option of increasing the magnetic field at the channel front is thus to implement stronger magnets.

The test data presented up to now were obtained with a fixed cathode mass flow rate of 5 sccm krypton (approximately 0.3 mg/s). However, the discharge behavior of hollow cathodes is tightly connected to the mass flow rate that is led through the cathode. Consequently, the influence of different cathode to total mass flow rate proportions was investigated. Figure 26 summarizes the discharge voltage and thrust for different cathode mass flow rate proportions at an operating point of 2 A with a total mass flow rate of 0.8 mg/s. While

the thrust is relatively unaffected by changes in the mass flow rate proportion, the keeper and discharge voltages differ depending on the ratio. Below 50% cathode proportion, both keeper and discharge voltage are approximately constant. At higher ratios, the keeper voltage slightly decreases, likely due to an increased cathode interior pressure which facilitates cathode operation. In contrast, the anode voltage slightly increases. Thruster operation at higher cathode mass flow rate ratios than 80% was not possible. To avoid the increase in discharge voltage and improve discharge stability, it is preferable to lead a majority of the gas through the main gas supply and minimize the cathode mass flow rate.

As thruster operation highly depends on the reliability of the hollow cathode, an investigation of different additives to the C12A7:e- emitter was conducted. As shown in Sect. 2.4, a higher molybdenum content in the emitter can alter the discharge properties of the insert. A comparison of the thruster performance for a 10 and 20% molybdenum content in the C12A7:e- emitters is shown in Fig. 27. Increasing the molybdenum content allowed to stably operate the thruster at discharge currents as low as 1 A. For currents between 2 and 3 A, the thrust and I_{sp} do not significantly vary with molybdenum content. The discharge voltage on

Fig. 26 Influence of cathode to total mass flow rate ratio on discharge voltage and thrust

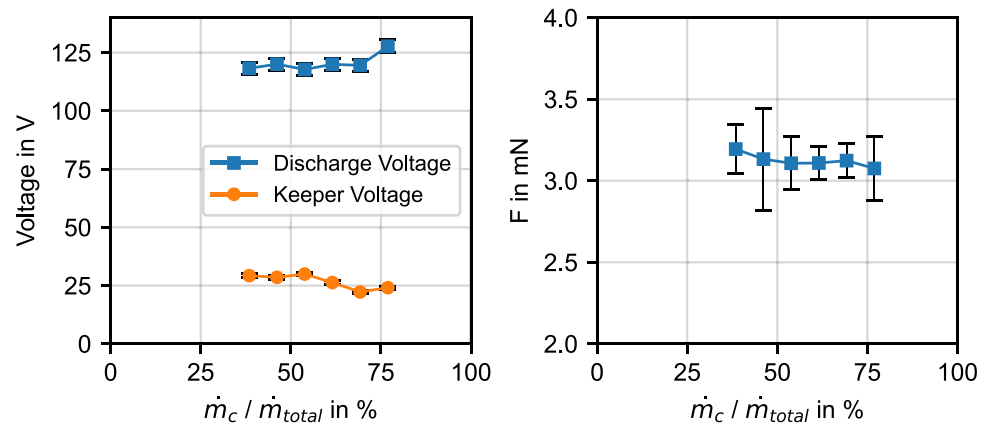
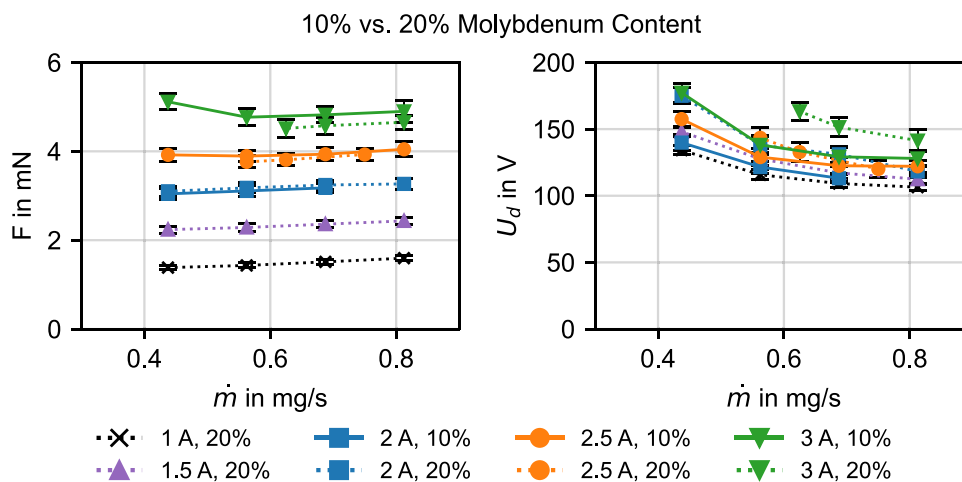


Fig. 27 Influence of emitter molybdenum content on thrust and discharge voltage



the other hand is notably increased using the higher molybdenum content, resulting in lowered overall efficiencies. This increase in discharge voltage could not be seen in the electrothermal thruster and might be attributed to other factors like the electrical connection using the silver adhesive. In general, operating the thruster over a wider current range is very advantageous for thruster scaling and to increase the span of achievable operating points.

The test series highlighted a distinct drawback of the prototype. Operating the thruster at currents of 2 A and above resulted in the visible glowing of the front anode segment, implying thermal problems. The temperature of the magnets during the test series was measured using a K-type thermocouple and did not show temperatures exceeding 50 °C, since the discharge for the individual operating points was only engaged for a maximum of 10 s to avoid overheating. Similarly, Ichihara et al. [27] also limited the maximum operational time of the thruster to a few seconds due to the lack of cooling. The thrust measurement signal did not show signs of a thermal drift, indicating that the high temperatures were concentrated at the anode segments. A long-term operation with the presented prototype without damaging individual components is nevertheless improbable and was not tested. The high anode temperatures clearly indicate high power losses from the plasma to the anode.

4 Conclusion

The presented electrothermal thruster concept is the most straightforward approach of using a hollow cathode as a stand-alone thruster. The tests proved the capability of the thruster to operate at a high micronewton to low millinewton thrust range. The maximum achievable I_{sp} was limited to sub-200 s in spot mode operation of the hollow cathode and the comparatively high discharge power resulted in sub—1% efficiencies. To increase the attractiveness of the

concept, a significant increase in discharge current and a decrease in discharge voltage would be necessary. A further increase in discharge current with the current emitter configuration likely poses a problem to the thermal constraints of C12A7:e-. The test results overall show that the use of C12A7:e- hollow cathodes in electrothermal devices cannot be recommended to date.

The MPDT concept showed the capability to operate in a low millinewton thrust range, an I_{sp} between 400 and 1191 s, and efficiencies up to 5.6%. The main problem with this concept is the high heat load on the anode, which likely limits the discharge current range to milliamps or low amps. The thruster performance shows a large discrepancy from the ideal electromagnetic thrust, which implies high power and particle momentum losses. The magnetic field in the presented prototype requires improvement to reduce the gradient towards the channel exit and increase the magnetic field in front of the orifice. The use of a multi-orifice keeper could be identified as an improvement in terms of thrust and I_{sp} compared to a single orifice keeper. The segmentation of the anode in the context of the presented test series is rudimentary and could not be investigated in detail due to test infrastructure constraints. Concluding from known MHD systems and the concept by Ichihara et al. [27], operating the thruster by taking advantage of the anode segmentation is beneficial and can increase the efficiency.

Acknowledgements This work has received funding from the European Unions Horizon 2020 research and innovation programme under grant agreement No 828902 (E.T.PACK project).

Funding Open Access funding enabled and organized by Projekt DEAL.

Open Access This article is licensed under a Creative Commons Attribution 4.0 International License, which permits use, sharing, adaptation, distribution and reproduction in any medium or format, as long as you give appropriate credit to the original author(s) and the source, provide a link to the Creative Commons licence, and indicate if changes

were made. The images or other third party material in this article are included in the article's Creative Commons licence, unless indicated otherwise in a credit line to the material. If material is not included in the article's Creative Commons licence and your intended use is not permitted by statutory regulation or exceeds the permitted use, you will need to obtain permission directly from the copyright holder. To view a copy of this licence, visit <http://creativecommons.org/licenses/by/4.0/>.

References

- Gondol, N., Tajmar, M.: Design of a hollow cathode thruster: concepts, parameter study and initial test results. *CEAS Space J* **14**, 65–77 (2021)
- Toda, Y., Matsuishi, S., Hayashi, K., Uedo, K., Kamiya, T., Hirano, M., Hosono, H.: Field emission of electron anions clathrated in subnanometer-sized cages in $[C_{24}Al_{28}O_{64}]^{4+}(4e^-)$. *Adv Mater* **16**(8), 685–689 (2004)
- Kim, S.W., Toda, Y., Hayashi, K., Hirano, M., Hosono, H.: Synthesis of a room temperature stable $12CaO \cdot 7Al_2O_3$ electride from the melt and its application as an electron field emitter. *Chem Mater* **2006**(18), 1938–1944 (2006)
- Toda, Y., Yanagi, H., Ikenaga, E., Kim, J., Kobata, M., Ueda, S., Kamiya, T., Hirano, M., Kobayashi, K., Hosono, H.: Work function of a room-temperature, stable electride $[Ca_{24}Al_{28}O_{64}]^{4+}(4e^-)$. *Adv Mater* **19**, 3564–3569 (2007)
- Drobny C, Wulfkühler J-P, Wätzig K, Tajmar M. Endurance test of a hollow cathode using the emitter material C12A7 electride. In: *SP2020-00153*, 2020+1. 2021.
- Gessini P, Gabriel SB, Fearn DG. The hollow cathode as a micro-ion thruster. In: *IEPC-01-233*, 27th International electric propulsion conference, 2001.
- Kameyama, I., Wilbur, P.J.: Measurements of ions from high-current hollow cathodes using electrostatic energy analyzer. *J Propul Power* **16**(3), 529–535 (2000)
- Patterson SW, Fearn DG. The generation of high energy ions in hollow cathode discharges. In: *IEPC-99-125*, 26th international electric propulsion conference, 1999.
- Gessini P, Gabriel S. Hollow cathode thrust measurement using a target: system development and calibration. In: *AIAA 2002-4104*, 38th AIAA/ASME/SAE/ASEE joint propulsion conference & exhibit, Indianapolis, Indiana, 2002.
- Gessini P, Gabriel S. Hollow cathode thrust measurements using a target: initial results and some issues. In: *IEPC-0253-0303*, 28th IEPC Toulouse, France, 2003.
- Gessini P, Gabriel S. Hollow cathode thrust measurements using a target. In: *4th International spacecraft propulsion conference*, Cagliari, Italy, 2004.
- Gessini, P., Coletti, M., Gabriel, S.: The thrust generated by a T6 ion engine hollow cathode. *Acta Astronaut* **102**, 249–257 (2014)
- Grubisic A. Microthrusters based on the T5 and T6 hollow cathode. PhD thesis, University of Southampton, 2009.
- Frollani D. Modelling and design optimisation of a hollow cathode thruster. PhD thesis, University of Southampton. 2014.
- Mikellides, I.G., Katz, I., Goebel, D.M., Polk, J.E.: Hollow cathode theory and experiment. II. A two-dimensional theoretical model of the emitter region. *J Appl Phys* **98**, 113303 (2006)
- Sary, G., Garrigues, L., Boeuf, J.-P.: Hollow cathode modeling: II. Physical analysis and parametric study. *Plasma Sources Sci Technol* **26**, 055008 (2017)
- Mikellides, I.G.: Effects of viscosity in a partially ionized channel flow with thermionic emission. *Phys Plasmas* **16**, 013501 (2009)
- Chu, E., Goebel, D.M.: High-current lanthanum hexaboride hollow cathode for 10-to-50-kW hall thrusters. *IEEE Trans Plasma Sci* **40**(9), 2133–2144 (2012)
- Goebel, D.M., Becatti, G., Mikellides, I.: plasma hollow cathodes. *J Appl Phys* **130**, 050902 (2021)
- Pedrini, D., Misuri, T., Paganucci, F., Andrenucci, M.: Development of hollow cathodes for space electric propulsion at sitael. *Aerospace* **4**(2), 26 (2017)
- Myers RM, Manteniaks M, LaPointe M. MPD thruster technology. In: *AIAA-91-3568*, conference on advanced space exploration initiative technologies, 1991.
- Fradkin, D.B., Blackstock, A.W., Roehling, D.J.: Experiments using a 25-kw hollow cathode lithium vapor MPD arcjet. *AIAA J* **8**(5), 886–894 (1970)
- Toki K, Shimizu Y, Kuriki K. Hollow cathode MPD thruster. In: *AIAA-85-2057*, *AIAA/DGLR/JSASS 18th international electric propulsion conference*, 1985.
- Toki K, Shimizu Y, Kuriki K. Electric propulsion experiment (EPEX) of a repetitively pulsed MPD thruster system onboard space flyer unit. In: *IEPC-97-120*, 1997.
- Toki K, Shimizu Y. Study of low-power MPD propulsion for future high-power trend. In: *AIAA 2002-4115*, 38th AIAA/ASME/SAE/ASEE joint propulsion conference & exhibit, 2002.
- Ichihara, D., Uno, T., Kataoka, H., Jeong, J., Iwakawa, A., Sasoh, A.: Ten-ampere-level, applied-field-dominant operation in magnetoplasmadynamic thrusters. *J Propul Power* (2016). <https://doi.org/10.2514/1.B36179>
- Ichihara, D., Harada, S., Kataoka, H., Yokota, S., Sasoh, A.: Operation characteristics of steady-state, applied field, rectangular magnetoplasmadynamics (MPD) thruster (in Japanese). *J Jpn Soc Aeronaut Space Sci* **63**(2), 37–44 (2015)
- Kodys AD, Choueiri EY. A critical review of the state-of-the-art in the performance of applied-field magnetoplasmadynamic thrusters. In: *AIAA-2005-4247*, 2005.
- Harada N, Ikewada J, Terasaki Y. Basic studies on an MHD accelerator. In: *AIAA-2002-2175*, 33rd plasmadynamics and lasers conference, Maui, Hawaii, 2002.
- Harada N. MHD acceleration studies at Nagaoka University of Technology. In: *AIAA-2001-2744*, 32nd AIAA plasmadynamics and lasers conference, Anaheim, CA, USA, 2001.

Publisher's Note Springer Nature remains neutral with regard to jurisdictional claims in published maps and institutional affiliations.